Proceedings of the Eighth International Conference on Cyclotrons and their Applications, Bloomington, Indiana, USA

STATUS OF THE KIEV 240-cm CYCLOTRON FACILITY

Yu.G. Basargin, V.A. Belyakov, V.A. Glukhikh, O.A. Gusev, L.E. Korolev,
R.N. Litunovsky, I.F. Malishev, O.A. Minyaev, A.V. Stepanov, A.S. Fedorov

D.V. Efremov Scientific Research Institute of Electrophysical Apparatus, Leningrad, USSR

A.F. Linev, A.I. Malofeev, O.F. Nemets, K.J. Ol'khovsky, V.A. Pashin

Nuclear Research Institute of the Ukrainian Academy of Sciences, Kiev, USSR

Abstract

The 240-cm isochronous cyclotron has been operating at the Kiev Nuclear Research Institute for two years. The present status of the accelerator is reported. The accelerated beam characteristics are given. The improvements from the moment the cyclotron was put into operation are described, and plans for further modifications are discussed.

* * * * * *

The 240-cm isochronous cyclotron of the Kiev Nuclear Research Institute operates in three independent modes. The first one is the "constant orbit" mode, where the following particles are accelerated:

1) protons with energy from 13 MeV to 80 MeV;
2) deuterons with energy from 20 MeV to 70 MeV;
3) $^4He^{+2}$ ions with energy from 20 MeV to 140 MeV;
4) $^3He^{+2}$ ions with energy from 45 MeV to 160 MeV.

The energy spread of the extracted cyclotron beam does not exceed 2×10^{-3} at the transverse emittance ~15π mm.mrad, the ion bunch time duration 5°-25° and the beam intensity from several μA to several tens of μA. The proton energy can be increased up to 100 MeV by using the valley coils. In the second mode the cyclotron is used as a pulsed neutron source and the protons are accelerated up to 100 MeV and deuterons up to 70 MeV. The time duration does not exceed 5°. Finally, the cyclotron can be used as a heavy ion source. The ion energy is up to 140 Z^2/A MeV.

A general view of the cyclotron is given in Fig. 1 Probes, collimators, and beam extraction system elements are shown. The general diagram of the accelerating chamber is given in Fig. 2, indicating its separate elements. The ion source is inserted through the top hole in the magnet yoke. The source and the puller are installed in the calculated position with line accuracy of 0.2 mm by means of a geodesic theodolite. The beam phase selection is accomplished by two collimators, installed at the first beam turns.

The only dee has a 180° angle. The frequency ranges from 7.5 MHz to 22 MHz. Frequency stability is 10^{-6}. The accelerating voltage amplitude is controlled within 20 kV (13 MeV proton energy) and 106 kV (80 MeV proton energy). The maximum amplitude voltage is 125 kV. The amplitude stability is kept at the 2×10^{-3} level by means of the automatic amplification control system and automatic frequency trimming in the resonance loop. To extract the beam the combined system is used, incorporating a 30° short electrostatic deflector ($E_{max} \approx 120$ kV/cm), a compensated current channel (ΔB_{max} = 2400 G, dB/dx = 200 G/cm), a focusing iron channel (ΔB_{max} = 5000 G, dB/dx = 500 G/cm), and a correcting electromagnet with dipole and quadrupole coils. General views of the extraction system elements are given in Figs. 3, 4, and 5.

Three-sector weak-spiral magnetic structure of the cyclotron is used. The air gap value is 237 mm between the flat sector surfaces and 537 mm in the valleys between the sectors. To decrease iron saturation and its influence upon the magnetic field characteristics, all the sector edges are made protruded. The maximum values of the flutter and the spiral angle are 0.4 and 45°, respectively. Maximum consumed power of the main coil is 200 kW. The maximum total supply power of the 15 pairs of the concentric coils is 550 kW. The long-term field level stability is 3×10^{-5}. Since the given magnetic field stability is insufficient for stable operation when using the beam at the remote target, the phase stabilization system of the accelerated beam is used in the 240-cm cyclotron as well. The bunch phase data are received from the capacitive phase transducer, and to control field level a 3 A special coil of low power is used.

Special attention is paid to elimination of the possible non-controlled first harmonic of the magnetic field.

The program providing the record and control of all field perturbation sources has been accomplished. This program includes the following:

(a) precise control of all stages of the magnet manufacturing and assembly (for the majority of dimensions the measuring accuracy is some hundredths of mm, for less important dimensions it is 0.1 mm);
(b) the development of differential technique of the magnetic field first harmonic measurement;
(c) field perturbation measurement;
(d) modification of the harmonic coil power supply to cancel mean magnetic field contributions, and application of separate control of the first harmonic amplitude and phase;
(e) the program development of the harmonic coil current calculation to achieve maximum approximation to the optimum law.

In the course of the 53 MeV energy proton beam experiments, attempts were made to optimize the beam extraction conditions by direct selection of the harmonic coil currents. The harmonic coil currents determined by the preliminary program calculation agree with maximum beam extraction efficiency.

The main beam characteristics have been determined in the course of experiments with the 53 MeV energy proton beam. Phase bunch duration is 55°. Small intensity losses at the first turns are explained by the fact that the essentially negative phase ions hit the dee. The beam height is 10-12 mm. Coherent vertical oscillations are not observed. After two collimators were installed, the phase bunch duration decreased to 10°-25°. The beam intensity losses depend to a great extent on the emission slit width of the ion source. For beam with phase duration less than 10°, the source slit width should not exceed 1 mm.

The first orbit geometry (location and width of separate peaks) determined by experiment (Fig. 6) is in good agreement with calculation data, taking into account the transverse and longitudinal emittance of the beam.

The radial oscillation amplitude determined experimentally is 2-4 mm for different conditions of phase selection.

The beam is extracted by precession with the radial oscillation swing in the resonance region $\nu_r = 1$. Extraction depends significantly on observing acceleration isochronism. With significant field misalignment, the extraction efficiency decreased from 70% to 40-50% due to mixing of the observed coherent oscillations with noncoherent ones having amplitudes up to 3 mm. The selective extraction nature is well illustrated in Fig. 7, where the resonance curve oscillograms I(δB) for the extracted beam at different amplitudes of the accelerating potential are shown. The sharp intensity peaks, corresponding to the optimum mode of the beam injection into the deflector channel, are seen. The required stability of the accelerating voltage amplitude is within 0.2-0.3%.

The beam intensity losses at extraction are fully determined by the part hitting the septum. Losses are not observed in the extraction and transport channel. The beam current density distribution behind the deflector, the current channel, the magnetic shield, and the inlet into the correction channel are shown in Fig. 8.

During 1976-1978 proton beams with energy of 13 MeV, 53 MeV, 72 MeV, and 80 MeV, deuteron beams with energy of 26 MeV, 50 MeV, and 64 MeV, and $^4He^{+2}$ ion beams with energy of 50 MeV, 105 MeV, and 130 MeV have been obtained. The following parameters of the extracted beam have been obtained for the typical modes:

1) Mean intensity: 10-20 μA;
2) Energy spread: 3×10^{-3};
3) Phase bunch duration: 10-15°;
4) Transverse emittance: 15π mm.mrad.

Research work is presently being conducted in the fields of nuclear physics, biology, and applied sciences.

New developments include modification of the power supply of the beam transport channel elements, automatic accelerator control, and the data acquisition system for experiments.

Fig.1. General view of the cyclotron

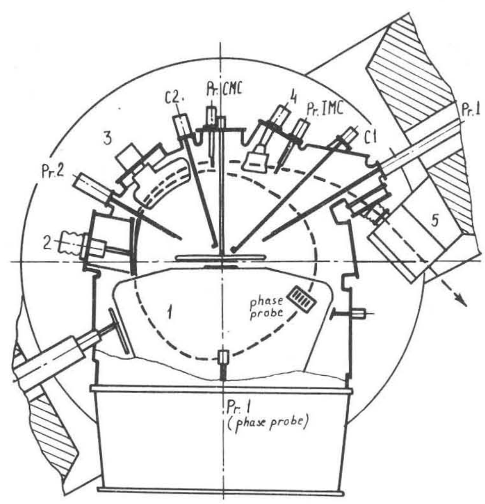

Fig.2. The diagram of the accelerating chamber: 1 - dee; 2 - electrostatic deflector; 3 - current channel; 4 - iron magnetic channel; 5 - correcting magnet

0018-9499/79/0400-1880$00.75

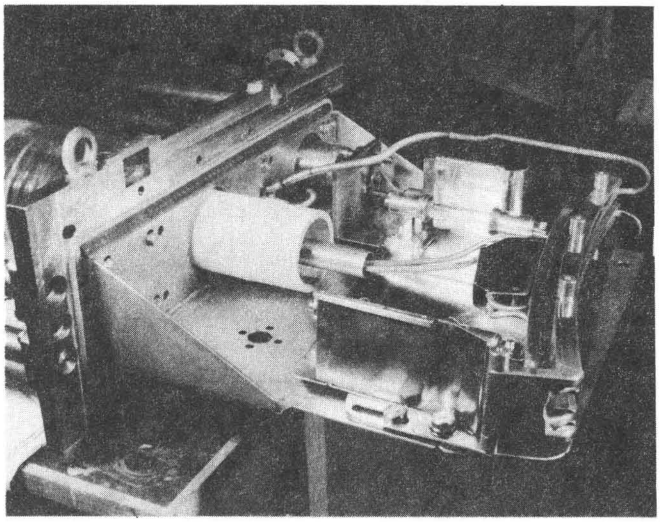

Fig.3. Electrostatic deflector

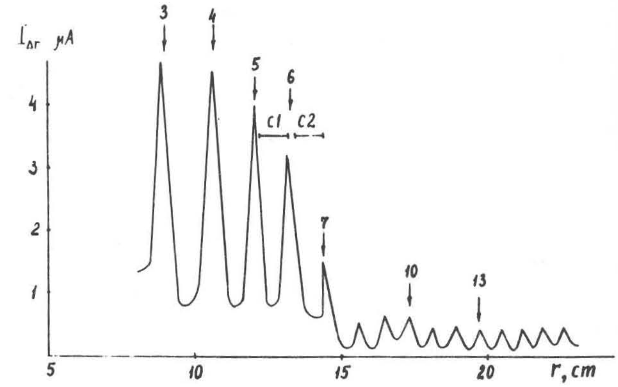

Fig.6. The beam current density at the first turns. The collimators C_1 and C_2 are installed

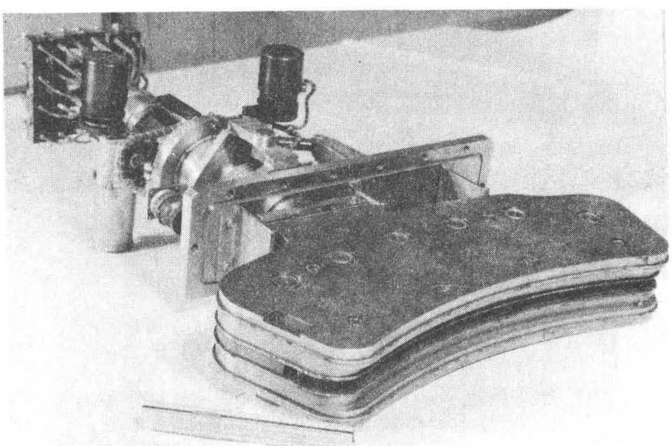

Fig.4. Current channel

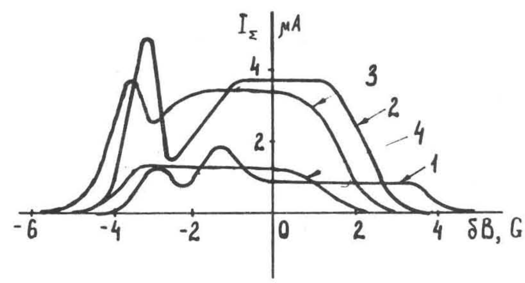

Fig.7. The resonance curve oscillograms for the extracted beam at different amplitudes of the accelerating potential:
1 - 81.3 kV; 2 - 76.7 kV;
3 - 74.2 kV; 4 - 72.2 kV

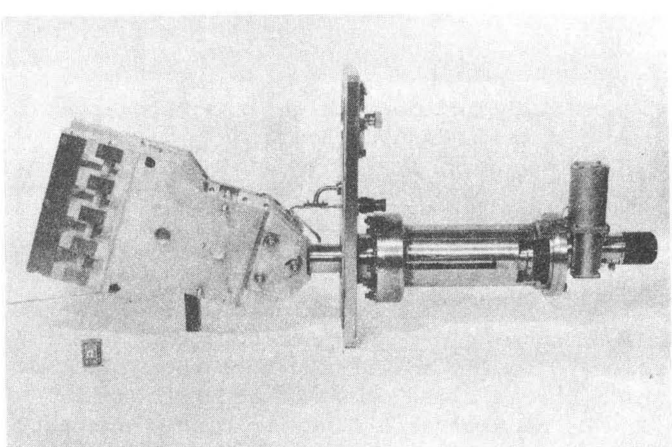

Fig.5. Iron magnetic channel

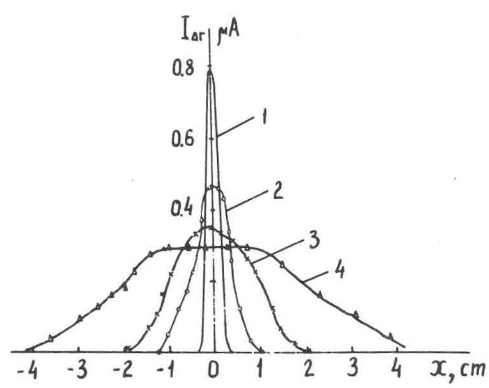

Fig.8. The current density distribution behind the deflector, the current channel, the magnetic channel and at the inlet into the correction magnet